Turbulent Impurity Transport Modeling for C-Mod and ITER

W. Horton 1), X. R. Fu 1), W. L. Rowan 1), I. O. Bespamyantnov 1),
S. Futatani 2), S. Benkadda 2), C. L. Fiore 3)

1) Institute for Fusion Studies, University of Texas at Austin, Austin, TX 78712, USA
2) CNRS-Université de Provence, FRANCE
3) MIT Plasma Science and Fusion Center, Cambridge, MA 02139, USA

email contact: wendell.horton@gmail.com

Abstract: Turbulent particle transport is investigated by analyzing recent boron impurity transport experiments in the Alcator C-Mod transport experiments with sets of partial differential equations (PDEs) for the multi-component plasmas. The PDE's give fast solutions for the fluctuation field vector composed of the electric potential ϕ, hydrogenic density δn_i and the impurity densities δn_{z1}, δn_{z2}. For comparison we carry out a limited number of simulations with the gyrokinetic code GTC. Linear eigenmode analysis shows that there are (1) the usual drift waves with hydrogen and the impurities convected by the dynamics of the TEM-ITG modes and (2) impurity drift waves supported by the impurity density gradients alone. The impurity drift waves add new degrees of freedom to the plasma allowing for hydrogen flux to be inward or outward. In these new modes the hydrogenic ions behave quasi-adiabtically since the parallel phase velocity is lower than in the TEM-ITG modes. The interaction between these two types of drift waves makes the transport matrix large and complex. We give examples for the particle fluxes for C-Mod in the H and ITB confinement modes. Related experiments reported on JET and TEXTOR are briefly discussed.

1. Introduction

Turbulent transport from drift waves is a key problem for fusion physics across all magnetic confinement geometries. To analyze plasmas with impurities a set of fluid equations are used to find the eigenmodes and eigenfrequencies of a nonuniform, magnetized plasma with a fluctuation vector $\mathbf{X_k}$ composed of fluctuations of the electron density, the working gas ion density, the impurity density and the electrostatic plasma potential. This structure of the eigenmodes and eigenvectors is shown for two collisionality regimes: (i) the collisional drift waves appropriate for the scrape off layer (SOL) and the edge plasma in limiter discharges and (ii) the trapped electron mode taken in the limit of a Terry-Horton[1] fluid description for the core plasma. From the eigenmodes and eigenvectors we compute the out-of-phase part of the density to potential fluctuations and analyze the quasilinear particle fluxes as a function of the power spectrum of the plasma potential fluctuations and the gradient parameters charactering the H and ITB confinement modes.

We use data from C-Mod experiments with boronized walls and with argon injection to obtain a wide range of plasma gradients and confinement regimes. Multiple types of drift wave modes exist in such plasmas. For each wave vector $\mathbf{k}$ there are one stable mode, one unstable mode and a third low-frequency damped parallel-ion-flow mode. In the nonlinear state, the modes are coupled in a complex manner. For weakly turbulent states, the quasilinear particle fluxes for hydrogenic and impurity gases are calculated

from the out-of-phase ϕ and δn_i and δn_z fluctuations. The qualitative changes of the particle fluxes with variation of the sign and strength of the density gradient lengths are compared with C-Mod plasmas in the H, and ITB mode regimes. Nonlinear simulations are carried out to study the change in the nature of the turbulence from boron to argon and with the change of plasma confinement regimes. Turbulence growth from initial plasma states with ($\delta n_e = \phi = 0$) and only a tiny injection of the impurity make clear the role of the impurity injection for drift wave dynamics. Both argon and boron ions can convect inward with velocities $v \sim D/L_{nz}$ for hollow impurity profiles.

From gyrokinetic equations we derive the Vlasov-Poisson dispersion relation with the impurities. We see there are three types of drift wave instabilities that produce turbulent particle and impurity fluxes: (1) the drift wave with hydrodynamic ion response giving ITG modes with quasi-adiabatic electrons, (2) the trapped particle mode-ITG mode (TEM-ITG) that has trapped electron resonances[2] and FLR-hydrodynamic ions and impurities, and (3) the impurity drift wave where the impurity has FLR-hydrodynamic response and the hydrogenic working gas has quasi-adiabatic response. The impurity mode is strongly unstable when the hydrogenic ions and the impurity ions have reversed (opposite direction) radial gradients and the turbulent flux then transports each ion type down its respective density gradient leading to a thorough mixing of the two ion types. This impurity mode requires that the impurity density component of $Z_{\rm eff}$ be of order unity. For a small impurity contribution to the effective charge the impurity drift mode is stable. Owing to the numerous parameters, the exact stability condition is complicated and must be determined numerically. We use Dtrans-Impure code which is available at `http://pecos.ph.utexas.edu/~vortex`.

To model the impurity mode turbulence we generalize the multi-fluid models given in Futatani et al[3, 4] so that the hydrogenic ion response has the quasi-adiabatic response

$$\frac{\delta n_i(k)}{n_i} = -\frac{e\phi_k}{T_i}\left(1 + \frac{ic_i(\omega_k - \omega_{*i})}{|k_\parallel v_i| + |\omega_{Di}|}\right) \tag{1}$$

where $c_i = \sqrt{\pi/2}$ and the frequencies ω_k, ω_{*i}, $k_\parallel v_i$ and ω_{Di} are defined in Sec. 2. This hydrogenic response is the ion analog of what is called the "i δ_k" response function used in the Terry-Horton model for TEM turbulence[1, 5].

While earlier studies suggest that the effect of heavy impurities is more dramatic on the fluctuations and transport than the lighter impurities we have not found a strong difference in the argon and boron dynamics in the C-Mod simulations. The difference in the fluxes is explained by the profiles of the impurities and the spatial distribution of the turbulence. The injection of argon at the edge of the plasma is widely considered as a method to create an edge localized radiation belt for a continuous heat exhaust lessening the thermal load on the divertor plates. This favorable role of impurities must be balanced with possible accumulation of impurities in the core plasma. There is a strict limit on the core impurity limit from radiated power losses and from D-T fuel dilution. From this perspective the use of low Z impurities including helium(He), carbon(C), beryllium(Be) is the better choice for impurity control of the burning plasma. For basically this reason the choice of the plasma facing components in the ITER machine [6] is beryllium.

For one impurity species there are four space-time fields of interest and the constraint of quasineutrality reduces the system to three free fields which are taken as the electron density, the hydrogenic ion density and the impurity density. The condition of quasineu-

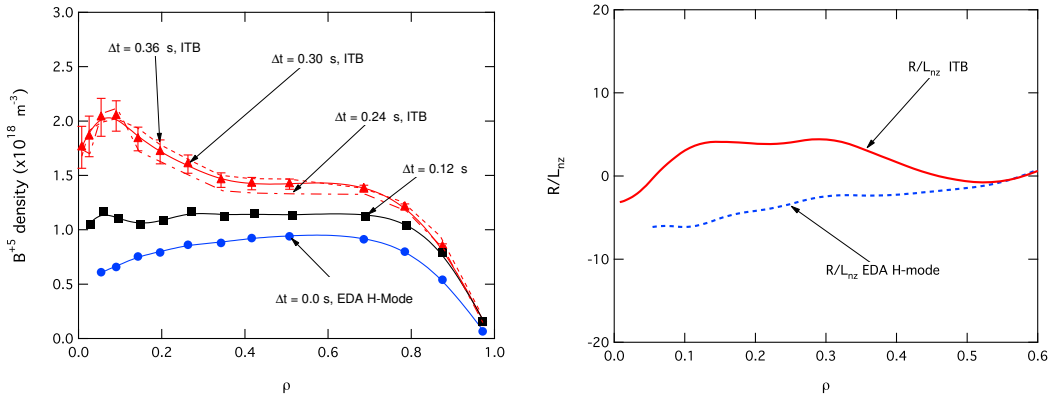

(a) (b)

FIG. 1. (a)Time evolution of boron density profile in the C-Mod discharge with 3.5 MW ICRF heating, from the H-mode (blue circles), transition (black squares), to ITB (red triangles); (b) boron density gradient profile in H-mode (blue dash) and ITB (red solid).

trality then determines the electrostatic field $\phi(x,t)$ and replaces the Poisson equation. Alternatively, one may view the three independent fields as the electrostatic potential ϕ, the ion density field n_i and the impurity density field n_z with the electron density determined by the quasineutrality condition

$$n_e(\mathbf{x},t) = n_i(\mathbf{x},t) + Zn_z(\mathbf{x},t). \tag{2}$$

We assume the plasma pressure-to-magnetic pressure ratio is sufficiently low that the electrostatic approximation is valid.

We show that the impurity gradient driven drift wave is unstable for the impurity profile peaked toward the plasma edge and produces inward transport of impurities and outward flux of hydrogen. This impurity drift wave rotates in the direction of the ion diamagnetic drift velocity. A similar result is reported in [7, 8] from quasilinear models. For pure hydrogen plasmas, the particle pinch term is inward for waves rotating in the ion diamagnetic direction, and outward for waves rotating in the electron direction. Generally, there are fluctuations rotating in both directions in a tokamak. By varying the ratio of the electron to ion thermal flux, Angioni et al [7] report a change from outward impurity flux for electron thermal loss dominated plasmas to the inward impurity pinch for ion thermal loss dominated plasma where the ITG modes rotate in the ion diamagnetic direction.

The confinement regimes are characterized by the plasma gradient parameters as follows: (1) H-mode the electron density profile is flattened and the low Z impurity profile is typically hollow. The hydrogenic profile is peaked on axis. We idealize this regime to have $\nabla(Zn_z + n_i) = 0$ so the theoretical model is taken as $R/L_{nz} = -6$ and $R/L_{ne} = 0$. The CXRS data confirms that the B^{5+} profile is hollow. (2) ITB internal transport barrier profiles have three radial subintervals: inside the barrier, in the barrier around $\rho = 0.5$ and outside the barrier. Inside the ITB we take $R/L_{nz} = 8$. Outside the ITB we take $R/L_{ne} = 4$ and $R/L_{nz} = 0$. Inside the transport barriers the particle dynamics is probably not diffusive and the transport model of [9, 10] may apply. This model has asymmetric left/right random steps.

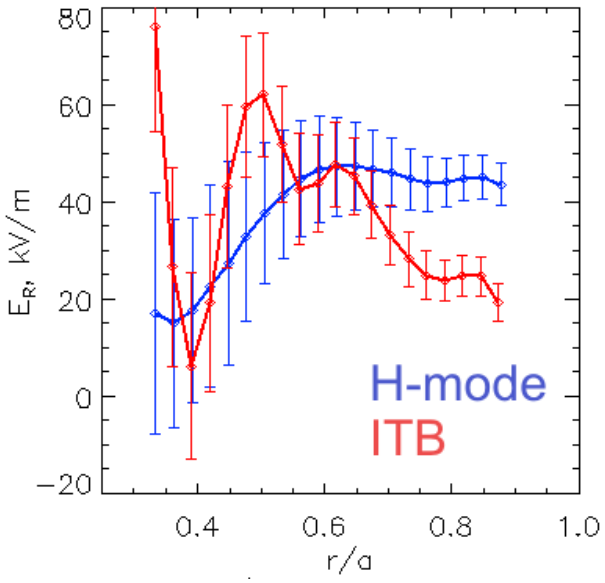

FIG. 2. The E_r profiles inferred from CXRS from Doppler shifts of boron lines used to compute the near to perpendicular boron flow velocity as given in Fiore et al [13]. The 20 ms profiles are given between the 200 msec interval before and after the transition from H mode (blue) to the ITB mode (red).

Rowan et al[11] show that the light impurity boron accumulates in the core of the ICRF driven ITB plasmas as had been shown earlier for argon in JET[12] and C-Mod. FIG. 1. shows the time evolution of the fully stripped boron from the H mode to the ITB. FIG. 1.(a) shows the change of the boron density profile from hollow at $t = 0$ (circles) through the transition with flat profile at $t = 0.12$ s (squares) to the peaked profile in the ITB regime $t = 0.24$ s to 0.36 s (diamonds). The normalized logarithmic gradient of boron density $n(\mathrm{B}^{+5})$ is shown in FIG. 1.(b) for the initial hollow profile in the H mode to the peaked profile in the ITB regime. The peak of the ICRF power deposition is at $\rho = 0.5$ just outside the ITB region which starts at $\rho = 0.4$. The interpretation is that the ITG-TEM modes are transporting the electrons and the boron inward with convection velocity $v = -Dr/a^2L_{nz}$. The change in the electron density profile from flat $R/L_{ne} \sim 0$ in the H mode regime to peaked $R/L_{ne} \sim 5$ in the ITB regime weakens the ITG and increases the density gradient driven TEM mode. The ITBs are created through a combination of strong E_r shear and control of the field line pitch giving locally weak or reversed magnetic shear. As shown in FIG. 2., the E_r shear in C-Mod experiments gives rise to the ITB.

TEXTOR-94 has $R/a = 1.75\,\mathrm{m}/0.46\,\mathrm{m}$ tokamak with circular cross section and limiter discharges. Typically the plasma has is flat topped for 4 seconds with four pulses of Argon at $t = 1, 2, 3, 4$ seconds. The XUX/VUV signals decay in 100 ms. The density is measured with interferometry and the $T_e(r)$ from ECE emission. The D and V values are inferred from simulations with all ionizations levels with the STRAHL transport code. To match the reported diffusivity of $D_{\mathrm{edge}} = 10\,\mathrm{m}^2/\mathrm{s}$ ($I = 301kA$) and of $D = 7\,\mathrm{m}^2/\mathrm{s}$ ($I = 447kA$), we use the qD_{gB} scaling as D_B/I_p. The level of fluctuations required is RMS $e\phi/T_e \sim 0.01$ with $k_y\rho_s = 0.3$. The associated pinch velocity is $-30\,\mathrm{m/s}$.

2. System of Gyrofluid Equations

The gyrofluid model for the drift wave turbulence is a simplified form of the Sugama-Watanabe-Horton equations for the density, parallel velocity and pressure for each species [14]. We consider the isothermal equation of state to eliminate the temperature gradient driven modes. Subscript s indicates species (e for electrons, i for ions, and $z1$ for first impurities, and $z2$ for second impurities). We use the nonlinear continuity equations for ions, impurities and electron and Ohm's law for parallel electron dynamics[15]. The drift frequency from the guiding center drift is a destabilizing effect with $\nabla \cdot \mathbf{v}_E = i\omega_{De} e\phi/T_e$, where $\omega_{De} = k_y(2cT_e/eBR)\cos\theta$. Here we define the diamagnetic drift frequencies

$$\omega_{*s} \;=\; k_y \frac{cT_s}{Z_s eB}\frac{1}{n_s}\frac{\partial n_{s0}}{\partial x} = -k_y\rho_s\frac{c_s}{L_{n_s}} \tag{3}$$

for $s = i$, $z1$, $z2$ and e.

2.1. Standard Drift Waves and Trapped Electron Mode

For the first model of drift wave impurity turbulence dimensionless partial differential equations are

$$\frac{\partial \tilde{n}_i}{\partial \tilde{t}} + \frac{R}{L_{n_i}}\frac{\partial}{\partial \tilde{y}}\tilde{\phi} + \left[\tilde{\phi}, \tilde{n}_i\right] - \left(\frac{\partial}{\partial \tilde{t}}\tilde{\nabla}_\perp^2\tilde{\phi} + \left[\tilde{\phi}, \tilde{\nabla}_\perp^2\tilde{\phi}\right]\right) = 0 \tag{4}$$

$$\frac{\partial \tilde{n}_z}{\partial \tilde{t}} + \frac{R}{L_{n_z}}\frac{\partial}{\partial \tilde{y}}\tilde{\phi} + \left[\tilde{\phi}, \tilde{n}_z\right] - \frac{A}{Z}\left(\frac{\partial}{\partial \tilde{t}}\tilde{\nabla}_\perp^2\tilde{\phi} + \left[\tilde{\phi}, \tilde{\nabla}_\perp^2\tilde{\phi}\right]\right) = 0 \tag{5}$$

$$\frac{\partial \tilde{n}_e}{\partial \tilde{t}} + \frac{R}{L_{n_e}}\frac{\partial}{\partial \tilde{y}}\tilde{\phi} + \left[\tilde{\phi}, \tilde{n}_e\right] + \frac{m_i}{m_e}\frac{c_s}{R\nu_{ei}}\tilde{\nabla}_\parallel(-\tilde{\nabla}_\parallel\tilde{n}_e + \tilde{\nabla}_\parallel\tilde{\phi}) = 0 \tag{6}$$

For linear analysis, we can assume fluctuation in the form of $\exp(i\mathbf{k}\cdot\mathbf{x} - i\omega t)$, drop nonlinear terms (Possion brackets), and rewrite linearized equations in the following matrix form

$$\mathbf{A}(\mathbf{k})\mathbf{X} = -i\omega\mathbf{B}(\mathbf{k})\mathbf{X}, \text{ where } \mathbf{X} = \begin{bmatrix} \frac{\delta n_i}{n_i} \\ \frac{\delta n_{z1}}{n_{z1}} \\ \frac{\delta n_{z2}}{n_{z2}} \\ \frac{e\phi}{T_e} \end{bmatrix} \tag{7}$$

The eigenvectors of the impurity drift wave matrix give the polarization of the fluctuations that determine the relative strength and direction of the hydrogenic and impurity ion transport. We can factor out X_4 which is $e\phi_k/T_e$ and write the new eigenvector as

$$\hat{\mathbf{X}}(\mathbf{k}) = \begin{bmatrix} \frac{\delta n_i}{n_e}/\frac{e\phi}{T_e} \\ \frac{\delta n_z}{n_e}/\frac{e\phi}{T_e} \\ \frac{\delta n_e}{n_e}/\frac{e\phi}{T_e} \\ 1 \end{bmatrix} \tag{8}$$

Physically, the $\hat{\mathbf{X}}$ vector describes the " polarization" of density waves related to the electrostatic wave. The particle fluxes are given by

$$\begin{aligned}
\Gamma_i &= \mathrm{Re}\sum_k \frac{ik_y\phi_k^*}{B}\delta n_i = -n_e\frac{T_e}{eB}\sum_k \frac{k_y|e\phi_k|^2}{T_e^2}\mathrm{Im}\hat{X}_1(k) \\
\Gamma_z &= \mathrm{Re}\sum_k \frac{ik_y\phi_k^*}{B}\delta n_z = -n_e\frac{T_e}{eB}\sum_k \frac{k_y|e\phi_k|^2}{T_e^2}\mathrm{Im}\hat{X}_2(k) \\
\Gamma_e &= \mathrm{Re}\sum_k \frac{ik_y\phi_k^*}{B}\delta n_e = -n_e\frac{T_e}{eB}\sum_k \frac{k_y|e\phi_k|^2}{T_e^2}\mathrm{Im}\hat{X}_3(k)
\end{aligned} \tag{9}$$

Quasineutrality gives $\Gamma_e = \Gamma_i + Z\Gamma_z$. The impurity flux is given by

$$\Gamma_z = -D_z\frac{\partial n_z}{\partial x} + V_z n_z \tag{10}$$

where

$$D_z = \sum_k \frac{v_x^2(k)\gamma}{B^2(\omega^2+\gamma^2)} \tag{11}$$

$$V_z = \sum_k \frac{v_x^2(k)\gamma}{\omega^2+\gamma^2}\left(\frac{\omega(k)eB}{k_yT_e}\right)k_\perp^2\rho_s^2 \tag{12}$$

The quasilinear formation in Eq. (9) is valid when there are overlapping resonants in the Hamiltonian motion of the test particles. In the nonlinear state the fastest growing modes couple to the damped eigenmodes driving them up to the level required for the power flow from the stable waves to balance the damping from the unstable modes.

The nonlinear waves saturate wave growth when the finite k_x part of the spectrum grows up to have the rms values of $\frac{\delta n_i}{n_i} \sim Z\frac{\delta n_z}{n_e} \sim \frac{\rho_\tau}{\langle k_x^2L_n^2\rangle^{0.5}}$. The spectrum has an isotropic part at higher $k_\perp$ and a zonal flow and density flattening part at low k_y values. There are coherent vortices that come and go in the turbulence which are especially strong in the limit of small parallel diffusivity $\nu_\parallel \ll |\omega_k|$. The spectral index $n = 3$ to 5 from simulations and scattering experiments. The turbulent wavenumber spectrum that enters Eq. 9 maybe modeled as

$$|\ \frac{e\phi_k}{T_e}\ |^2 = \frac{\rho_\tau^2}{L_n^2}\frac{1}{(1+k_\perp^2\rho_s^2)^{n/2}}. \tag{13}$$

where L_n is the dominant gradient scale length driving the growth rate. The dispersion relation, obtained by taking the determinant in Eq. (7) to be zero, gives

$$D^{\mathrm{DW}} = \omega^2(A\omega^2 + B\omega + C) = 0 \tag{14}$$

where $A = k_\perp^2\rho_s^2n_\tau$, $B = i[k_\perp^4\rho_s^2\mu_\tau + \nu_\parallel(1+k_\perp^2\rho_s^2n_\tau) + i\omega_{De}k_\perp^2\rho_s^2n_\tau]$ and $C = -(k_\perp^4\rho_s^2\mu_\tau + i\omega_{*e})(\nu_\parallel + i\omega_{De})$. There are two zero frequency modes and two non-zero roots of Eq. (14). We can estimate corresponding growth rates and frequencies provided $\omega_{De} = 0$, zero visicosities and $\gamma \ll \omega_r$.

$$\omega_r = \frac{\omega_{*e}}{1+k_\perp^2\rho_s^2n_\tau},\ \gamma = \frac{\omega_{*e}^2k_\perp^2\rho_s^2n_\tau}{(1+k_\perp^2\rho_s^2n_\tau)^2\nu_\parallel} \tag{15}$$

The trapped electron mode[3] can be solved similarly.

2.2. Impurity Drift Mode

The zero eigenvalues can be removed if we consider low-frequency acoustic waves. Consider the parallel force balance for ions and substitute parallel ion velocity $v_{i\|}$ into the continuity equation, we can get a new term

$$\nabla_\| v_{i\|} = -\frac{c_s^2}{\nu_i}\nabla_\|^2\left(\frac{e\phi}{T_e}+\frac{T_i}{T_e}\frac{\delta n_i}{n_i}\right) = \nu_{\|i}\frac{e\phi}{T_e}+\nu_{\|i}\frac{T_i}{T_e}\frac{\delta n_i}{n_i} \tag{16}$$

Similar terms apply added for impurities. The adiabatic electrons response $\delta n_e/n_e = e\phi/T_e$ occurs when $\nu_{\|e}\to\infty$. For $\nu_{\|z1},\nu_{\|z2}\sim 0$, the ion response is

$$\frac{\delta n_i}{n_i} = \left(\frac{i\omega_{*i}+i\omega k_\perp^2\rho_s^2-\nu_{\|i}}{-i\omega+\nu_{\|i}T_i/T_e}\right)\frac{e\phi}{T_e} \tag{17}$$

When $\nu_{\|i}\to\infty$, ions are adiabatic, i.e. $\delta n_i/n_i = -e\phi/T_i$; when $\nu_{\|i}\to 0$, ions are hydrodynamic, $\delta n_i/n_i = -(\omega_{*i}/\omega)(e\phi/T_i)$ giving the standard drift waves.

Now for $Z^2 n_z/n_e \lesssim 1$, we derive the impurity drift waves(IDW). The impurity drift wave has $|\omega|\ll\nu_{\|i}$ with the growth rate given by

$$\gamma_{\mathbf{k}}^{\mathrm{IDW}} = \frac{\frac{n_i}{n_e}\frac{T_e}{T_i}\frac{1}{\nu_{\|i}}\left[-\omega_{*i}+\omega(k_\perp^2\rho_s^2+T_e/T_i)\right]\left(Z_1\frac{n_{z1}}{n_e}\omega_{*z1}+Z_2\frac{n_{z2}}{n_e}\omega_{*z2}\right)}{\left[1+\frac{n_i}{n_e}\frac{T_e}{T_i}+k_\perp^2\rho_s^2(A_1\frac{n_{z1}}{n_e}+A_2\frac{n_{z2}}{n_e})\right]^2} \tag{18}$$

The impurity drift wave is unstable when $\omega_{*i}\omega_{*z}<0$.

3. Gyrokinetic Dispersion Relation

The GTC code[16] solves for the gyrokinetic distribution function given by

$$\delta f_s(k,\omega,v) = e\phi_k\left[\frac{\partial f_s}{\partial\epsilon}-\frac{\omega\frac{\partial f_s}{\partial\epsilon}+\frac{k_y}{e_sB}\frac{\partial f_s}{\partial x}}{\omega-\omega_{Ds}-k_\| v_\|}J_0^2(\frac{k_\perp v_\perp}{\omega_{cs}})\right] \tag{19}$$

where $\omega_{Ds}=\frac{k_y cT_s}{e_sBR}\left(\frac{m_s v_\perp^2}{2T_s}+\frac{mv_\|^2}{T_s}\right)$ with $s=e,i,z$ for electron, ion and impurity species. In the quasineutral limit with a local Maxwell-Boltzman distribution, the analytic dispersion relation is

$$D^{\mathrm{GTC}}(\omega,k) = \sum_j\frac{Z_j^2 n_j e^2}{T_j}\left[1-\langle\frac{\omega-\omega_{*j}(1+\eta_i(\epsilon-3/2))}{\omega-\omega_{Dj}-k_\| v_\|}J_0^2\rangle_M\right] \tag{20}$$

where the $\langle g\rangle_M$ denotes the average over the Maxwell-Boltzmann.

For ITG modes with adiabatic electrons we find both the hydrogen and impurity temperature gradients driven the turbulence. When the density gradient is less than the temperature gradient we find the instability condition

$$\frac{n_iT_e}{n_eT_i}\frac{R}{L_{Ti}}+\frac{Z^2n_z}{n_e}\frac{T_e}{T_z}\frac{R}{L_{Tz}} > 1+\frac{T_e}{T_i}(1-f_z)+\frac{T_e}{T_z}\frac{Z^2n_z}{n_e} \tag{21}$$

For inverse cascade to wavelength $k_y\rho_s = L_T/qR$ we find the turbulent diffusivity scales as

$$D^{\rm ITG} = {\rm Const}\left(\frac{T_e}{eB}\right)\left(\frac{q\rho_s}{L_{T_i}}\right)\left(1 - f_z + \frac{L_{Ti}}{L_{Tz}}\frac{Z^2 n_z}{n_e}\right)^{1/2} \tag{22}$$

where $T_z = T_i$ and $L_{Ti} \approx L_{Tz}$. Simulations with GTC are being carried out to test the scaling with the impurities.

4. Conclusions and Application to ITER

We have written and are running subroutines for solving systems of drift wave turbulence equations for the multi-component fusion plasmas. The subroutines are fast compared with gyrokinetic simulations and suitable for near-to-real time analysis of tokamak data. Typical values for the ITER plasma assuming a 3% beryllium corresponding to a charge fraction $f_Z = Zn_z/n_e = 48\%$ and a $Z_{\rm eff} = 2$. The initial findings for the characteristics of the impurity transport are that there is an inward transport of beryllium to the core of the H-mode plasma similar to that of boron in the C-Mod experiments. For the model values we estimate a $D_{ne} = 3\,{\rm m}^2/{\rm s}$ and $D_{nz} = 5\,{\rm m}^2/{\rm s}$ for the core and $D_{ne} = 6\,{\rm m}^2/{\rm s}$ and $D_{nz} = 6\,{\rm m}^2/{\rm s}$ for the edge plasma. In the H-mode we estimate $v_z = -D_{nz}(\rho_s/L_{nz})^2$ for the pinch velocity.

Acknowledgements

This work was supported by Department of Energy, US DoE award DE-FG03-96ER54373, the Center for Turbulence at the Universite of Provence, Marseille and the CEA at Cadarache.

References

[1] TERRY P. W., HORTON, W., *Phys. Fluids*, **26**, 106 (1983).
[2] KADOMTSEV, B. B., POGUTSE, O. P. *Nucl. Fusion*, **11**, 67 (1971).
[3] FUTATANI, S., et al., *Physics of Plasmas* **17**(2010).
[4] DUBUIT, N., et al., *Phys. Plasmas*, **14**, 042301 (2007).
[5] HORTON, W., ICHIKAWA, Y.-H. *Chaos and Structures in Nonlinear Plasmas*, World Scientific, Singapore(1996).
[6] BROOKS, J. N., et al., *Nucl. Fusion*, **49**, 035007 (2009).
[7] ANGIONI, C., et al., *Nucl. Fusion*, **49**, 055013 (2009).
[8] HORTON, W., *Phys. Fluids*, **19**, 711 (1976).
[9] DEL-CASTILLO-NEGRETE, D., et al., *Phys. Plasmas*, **11**, 3854 (2004).
[10] KWON, J-M., et al., *Phys. Plasmas*, **7**, 1169 (2000).
[11] ROWAN, W. L., et al., *Nucl. Fusion*, **48**, 105005 (2008)
[12] DIETZ, K. J., et al., *Plasma Physics and Controlled Fusion*, **32**, 837 (1990).
[13] FIORE, C. L., et al., *Nuclear Fusion 12th International H-Mode Workshop Special Issue*, 2010
[14] SUGAMA, H., et al., *Phys. Plasmas*, **14**, 022502 (2007)
[15] HASEGAWA, A., WAKATANI, M. *Phys. Rev. Lett.*, **50**, 682 (1983).
[16] HOLOD, I., et al. *Phys. Plasmas*, **16**, 122307(2009).